Pain Medicine, 2023, **24**, 528–537
https://doi.org/10.1093/pm/pnac205
Advance access publication 30 December 2022
Original Research Article

OXFORD

PSYCHOLOGY, PSYCHIATRY & BRAIN NEUROSCIENCE SECTION

Detangling the Structural Neural Correlates Associated with Resting versus Dynamic Phantom Limb Pain Intensity Using a Voxel-based Morphometry Analysis

Camila B. Pinto, PhD,[1] Kevin Pacheco-Barrios, MD,[1,2] Faddi G. Saleh Velez, MD,[3] Muhammed E. Gunduz, MD,[1] Marionna Münger, MSc,[1] Felipe Fregni, MD, PhD[1,*]

[1]Neuromodulation Center and Center for Clinical Research Learning, Spaulding Rehabilitation Hospital and Massachusetts General Hospital, Harvard Medical School, Boston, MA 02129, United States,
[2]Universidad San Ignacio de Loyola, Vicerrectorado de Investigación, Unidad de Investigación para la Generación y Síntesis de Evidencias en Salud, Lima 01425, Peru,
[3]Department of Neurology, University of Chicago Medical Center, University of Chicago, Chicago, IL 60637, United States

C.B.P. and K.P.-B. contributed equally.

**Corresponding author:* Neuromodulation Center and Center for Clinical Research Learning, Spaulding Rehabilitation Hospital and Massachusetts General Hospital, Harvard Medical School, 96 13th Street, Charlestown, Boston, MA 02129, USA. Email: Fregni.Felipe@mgh.harvard.edu

Abstract

The management of phantom limb pain (PLP) is still challenging due to a partial understanding of its neurophysiological mechanisms. Structural neuroimaging features are potential biomarkers. However, only a few studies assessed their correlations with clinical severity and treatment response. This study aims to explore the association between brain gray matter volume (GMV) with phantom limb manifestations severity and PLP improvement after neuromodulatory treatments (transcranial direct current stimulation and mirror therapy). Voxel-based morphometry analyses and functional decoding using a reverse inference term-based meta-analytic approach were used. We included 24 lower limb traumatic amputees with moderate to severe PLP. We found that alterations of cortical GMV were correlated with PLP severity but not with other clinical manifestations. Less PLP severity was associated with larger brain clusters GMV in the non-affected prefrontal, insula (non-affected mid-anterior region), and bilateral thalamus. However, only the insula cluster survived adjustments. Moreover, the reverse inference meta-analytic approach revealed that the found insula cluster is highly functionally connected to the contralateral insula and premotor cortices, and the decoded psychological processes related to this cluster were "rating," "sustained attention," "impulsivity, " and "suffering." Moreover, we found that responders to neuromodulatory treatment have higher GMV in somatosensory areas (total volume of S1 and S2) in the affected hemisphere at baseline, compared to non-responders, even after adjustments.

Keywords: Phantom limb pain; neuroimaging; voxel-based morphometry; biomarkers; predictors

Perspective

Our results suggest an essential role of the non-affected mid-anterior insula as an integrating hub of PLP perception and its severity and thus being a critical network for resting PLP intensity. On the other hand, the sensorimotor gray matter volume seems to be critical to ultimately influence the likelihood of dynamic PLP intensity changes related to a neuromodulatory treatment aimed at sensorimotor cortex modulation. These results point out to the importance in differentiating resting vs. dynamic structural brain correlates associated with PLP control.

Introduction

In the United States, nearly 185 thousand people undergo an amputation each year [1], and it is estimated that 64% of them will potentially developed phantom limb pain (PLP) [2]. PLP is the perception of pain in a limb that is no longer there, most commonly as a sequela of amputation [3].

The current common management approaches include analgesics (of opioid and non-opioid nature), physical therapy, or complementary interventions such as mirror therapy, biofeedback, and chiropractic care [4]. However, several patients reported worsening of their symptoms after these interventions [5]. Thus, despite a large quantity of available approaches, the management of PLP is still extremely challenging [6, 7].

A major difficulty in developing targeted PLP treatments stems from partial understanding of its neurophysiological mechanisms. The presence of PLP after amputation has been associated with cerebral, spinal, and peripheral changes [6]. The most commonly reported are somatosensory cortex, motor cortex, and thalamic alterations, indexed by magnetic resonance imaging (MRI) [8], functional MRI (fMRI) [9, 10], and transcranial magnetic stimulation (TMS) [11, 12]. Specifically, PLP has been associated with altered persistence of the cortical representation of the amputated limb [10], motor cortex disorganization (12), sensorimotor cortex hyperactivity (13), and hyperconnectivity between insula and sensorimotor cortices (S1/M1) (13).

Received: April 2, 2022. **Revised:** September 23, 2022. **Accepted:** October 20, 2022

Several potential biomarkers had been used to understand the pathophysiology of PLP, although they have yielded heterogeneous results. The brain volumetric difference of gray matter is a promising and reliable neuroimaging feature that could be used to understand neuroplasticity characteristics of neuropsychiatric diseases [14], and had been shown altered in chronic pain populations [15, 16]. Nevertheless, only few studies used this methodology in PLP patients in the past [17–20]. Draganski et al. (2006) assessed brain volumetric differences in 28 amputees with PLP compared to 28 matched healthy controls. They found that PLP patients had less gray matter in the contralateral thalamus, and these changes were mediated by the time since amputation (PLP chronicity was associated with smaller thalamic volume); however, no volumetric changes were associated with PLP severity [17]. Similarly, Preissler et al. (2013) found that amputees with PLP compared to healthy participants had reduced global gray matter, especially in the motor cortex and right dorsolateral pre-frontal cortex. Additionally, the subjects with high PLP have higher gray matter volume in the left anterior cingulate cortex and less volume in pain processing areas, compared to subjects with mild/non-existent PLP [19].

The previous explorations were mainly restricted to the comparison between amputees and healthy controls and including heterogenous samples. Nevertheless, the brain volumetric correlates of clinical severity assessments (PLP, depression, and anxiety severity) and its predictive value for treatment response were not consistently explored. Thus, the structural neuroimaging correlates of clinical severity in PLP patients are mostly unknow, despite being severity highly influential on the patient's quality of life [21]. Moreover, it is unclear which structural neuroimaging markers can predict PLP reduction after treatment, which is a needed information to implement a personalized management approach in PLP [22].

This study aims to explore the association between brain gray matter volume (GMV) and phantom limb manifestations severity in lower limb traumatic amputees with PLP. Additionally, we assessed whether gray matter volume at baseline can predict PLP reduction after a neuromodulatory treatment (transcranial direct current [tDCS] stimulation and mirror therapy). We hypothesized that PLP intensity at baseline will be associated with differences in GMV of pain-related areas such as sensorimotor cortex, thalamus, cingulate cortex, insula, and pre-frontal region. Furthermore, we hypothesized that treatment response to neuromodulatory interventions will be associated with differences in GMV of the target stimulation region (sensorimotor cortex).

Methods

Study design

A secondary analysis was performed utilizing data from a double-center, placebo controlled, randomized clinical trial (NCT02487966) [23] that assessed the effects of the combination of Mirror therapy and tDCS for the relief of phantom limb pain in lower limb traumatic amputees. The details of the rationale, design and methods of the source study as well as the results are published elsewhere [23, 24].

Informed consent was obtained prior to the enrollment and the study was approved by Partners Institutional Review Board (Spaulding Rehabilitation Hospital) and the University of Sao Paulo Institutional Review Board accordingly. The complete methodology of this trial was published elsewhere [23]. The STROBE statement was followed for reporting this study (supplementary material).

Participants

The source study was composed of 132 participants. For the purpose of this analysis, 24 subjects enrolled at the Boston University neuroimaging center were included, since not all enrolled participants underwent MRI procedures. Included patients had moderate to severe PLP (>4 in VAS).

Clinical and demographic variables

Demographic questionnaire

Demographic variables such as gender, ethnicity, age, and study center were collected.

Amputation-related variables

An adapted version for lower limb amputation [25] of the "Groningen questionnaire after arm amputation" was used to collect relevant data regarding the amputation (ie, laterality of amputation, amputation level, previous treatment, opioid use). Also, we collected the severity of PLP, phantom limb sensation (PLS), and residual limb pain (RLP) using a 0–10 VAS scale.

Other clinical variables

To address the psychological wellbeing of the subject data, the Beck depression index (BDI) and Beck anxiety index (BAI) were collected. We assessed the presence and degree of severity of depression and anxiety symptoms.

MRI acquisition and processing

Acquisition

The structural MRI was performed twice during the protocol (Figure 1) [23]. To scan all subjects we used a 3 Tesla Philips Achieva Scanner Center (Philips Medical Systems, Eindhoven, The Netherlands) located at the Center for Biomedical Imaging (CBI) at the Boston University Medical Center. A turbo spin echo sequence (time to echo [TE] = 3.1 ms, repetition time [TR] = 6.8 ms, flip angle = 9, voxel size 0.98_0.98_1.20 mm, no slice gap, acquisition matrix 256_254) was used to obtain anatomical T1-weighted images.

Voxel-based morphometry

The "Oxford Centre for Functional MRI of the Brain (FMRIB) Software Library" (FSL) v6.0 was used (FSL) [26]. We used FSL voxel-based morphometry (VBM) to analyze gray matter (GM) [27]. First, all images were stripped from the skull using Brain Extraction Tool (BET), visual quality control was performed before tissue-type segmentation into GM, white matter, and cerebrospinal fluid using the FMRIB's Automated Segmentation Tool (FAST) [27]. Second, we created two groups of analysis, one group for a non-flipped analysis and a second group in which brain images from left limb amputees were flipped along the *x*-axis (12 subjects); therefore, in all amputees the right cerebral hemisphere corresponds to the non-affected hemisphere. The main analysis was performed in the flipped brain and the non-flipped analysis was used a secondary quality control.

Third, we created a study-specific GM template using the 24- GM-segmented images—FAST. Steps toward the template

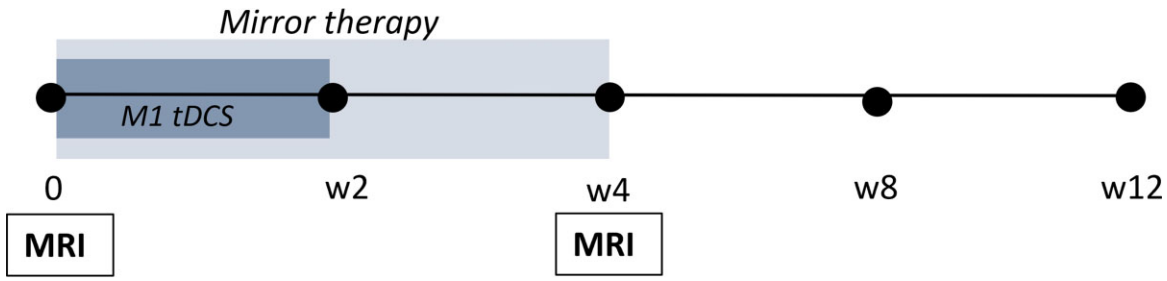

Figure 1. Study timeline and MRI acquisition timepoints. MRI was performed at baseline and after treatment. The intervention consisted in motor cortex transcranial current stimulation (M1 tDCS) for 2 weeks (10 sessions, weekdays) combined with 4 weeks of concomitant mirror therapy.

creation included: ine registering of the GM partial volume images (FLIRT) [28] and left-to-right *x*-axis flipping to produce a symmetrical image followed by nonlinear registration (FNIRT) [29] to standard space. The native space GM volume images were then normalized into this template using a nonlinear registration (FNIRT) and corrected for the contraction/enlargement due to the nonlinear component of the transformation using Jacobian integration.

Lastly, GM images were concatenated and smoothed with an isotropic Gaussian kernel (FWHM 3 mm). Gray matter volume associations with clinical variables were assessed using a correlation analysis using age, sex, and total intracranial volume (TIV), categorical variable for flipped data analysis as covariates of no interest. For cluster definitions we used the threshold-free cluster enhanced (TFCE) method. The TFCE images can easily be used to estimate statistical significance by calculating voxel wise *P* values (uncorrected or corrected for multiple comparisons across space) via permutation test. FSL's randomize toolbox [30] was used to perform the permutation-based testing (n = 5000 permutations) and to obtain threshold-free cluster enhanced (TFCE) uncorrected and corrected *P* values [31]. For the uncorrected *P* values a threshold of $P <= .001$ was used for statistical significance of associations. A minimum cluster size of 27 voxels (number of voxels contained within the 3 mm smoothing kernel- $3 \times 3 \times 3$) was used as a secondary threshold for the uncorrected [32].

Total gray matter volume estimation SIENAx (2.6) from FSL was used to calculate estimates of volumes of interest, after automated brain extraction and tissue segmentation [33]. Anatomical locations of significant clusters were determined using their MNI coordinates in MRIcron and xjview using the AAL template.

Neurosynth activation mask and decoding

Neurosynth is a public database that lists the results from >14000 functional MRI published investigations (https://neurosynth.org/). Neurosynth platform utilizes text-mining, machine learning and meta-analytic methods to generate automated large-scale analysis of neuroimaging [34]. This tool allows for tagging individual studies with all words that occur at least once in its abstract, excluding "stop words" and words that occur in more than 60% of all abstracts; therefore, studies can be retrieve using a specific term.

We used Neurosynth to create an activation mask based on the terms "hand" and "foot," by simply typing the term "hand" a statistical map of an automated meta-analysis was generated. For instance, the term "hand" retrieved 879 studies, while the term "foot" retrieved were 83 studies. We constructed the mask using additional synonyms as arm, leg, extremities, and limb. Using Neurosynth we were able to create a generalizable mask, dependent on the activation of this regions in several studies, instead of using only an atlas generate mask. We used a T-threshold of 5.5 and exported these maps into NIFTI format, where they were used in further analysis as ROI masks [34].

Besides the creation of the activation mask, Neurosynth can be queried for the functional decoding of voxel locations in MNI space [34]. For this task we used Neurosynth Decoder function to retrieve the probability of observing the reporting of a term given a particular location. In this case, the clusters AIs ROI were inputted and used to generate the semantic annotation of studies in the Neurosynth dataset that report this same region. This method allows the identification of terms that are most probably associated with specific brain images. We uploaded them individually. The relative similarities between the terms and VBM result images were shown in a rank order of correlation, then we created a word-cloud weighted so that the size reflects the highest correlation of the 20 first terms and each specific cluster.

Statistical analysis

Statistical analyses of GMV properties were performed using tools from the Oxford Center for Functional Magnetic Resonance Imaging Software Library (FMRIB, Oxford OK; FSL version 5.0.10, https://fsl.fmrib.ox.ac.uk/fsl). We reported the baseline characteristics using central tendency and dispersion measurements based on the variable type (eg, mean and SD for continuous variables, frequency tabulations for categorical variables). We used complete case analysis to manage missing data. To compare clusters, we used Mann-Whitney *U* tests. To understand the relationship of GMV and the clinical variables, Spearman's rank and Pearson's correlation tests were performed. To compare GMV values at baseline between responders (decrease of at least 30% of pain [35]) and non-responders, we used an unpaired *t*-test adjusted for age, gender, TIV, and flipped hemisphere. The statistical analyses were performed with Python version 3.9.

Results

Demographic characteristics

Twenty-four subjects were included in the VBM analysis, all from the Boston site. The sample was 58% male and the mean age of the participants was 51.79 (SD = 14.04 years). The median time since amputation was 21 months (IQR: 5.5 to 188), mean PLP, PLS, and RSL were 5.3 (SD = 1.72), 3.40 (SD = 2.90), and 5.08 (SD = 3.43), respectively. Further clinical data related to the amputation are provided in Table 1.

Structural gray matter volume and phantom limb pain intensity

First, we set up a statistical model to identify significant clusters that are correlated with phantom limb pain at baseline (age, gender, and TIV) and flipped them as covariates of no interest. All brains images were flipped across the midsagittal plane for left limb amputees (12 subjects), such that the left cerebral hemisphere would correspond to body side of the amputation to all patients. Two contrasts were tested, one contrast was performed for the positive correlations and the other for the negative correlations of GM volumes and PLP. Overall, five clusters were identified using a TFCE uncorrected *P* values binarized mask at a value of .001 and a cluster size >27 voxels (Table 2 and Figure 2 uncorrected T-maps) all for the second contrast. This indicated that more volume of the whole brain average was correlated with less pain (Figure 2 and Table 2).

We also evaluated the GM properties of these clusters across different demographics and pain characteristics (Figure 2C). Interestingly all regions significantly associated with PLP were not correlated with other phantom limb related syndrome such as phantom limb sensation and stump pain. Additionally, there was no significant correlation with GM volume and time since amputation, or depression and anxiety measurements.

Moreover, we use the same model in the non-flipped brain images and observed similar results. Five clusters were identified using a TFCE uncorrected *P* values binarized mask at value of .001 and cluster size >27 voxels all for the second contrast, indicating that more volume of the whole brain average was correlated with less pain. As expected, Insula and Frontal Lobe (dorsomedial pre-frontal cortex and subcallosal cortex) clusters—left and right also appeared in the non-flipped analysis results. The non-flipped analysis clusters considerably overlapped (Sørensen–Dice coefficient 5: 0.71) with the five clusters obtained in the flipped analysis. Overall, by aligning the brain in relation to body side of the amputation, we observed more statistically significant clusters and a stronger correlation of GM volume differences with the phantom limb pain.

Moreover, the Insula cluster on the non-affected hemisphere survived TFCE correction (Figure 2) and showed to be highly correlated with PLP intensity, at the same way the insula volume was not correlated with other phantom limb phenomena (PLS or RLS) or with time since amputation. This suggested that the changes in the insula volume are specific to pain. No gray matter volume differences at any brain area were associated with PLS or RLS intensities.

Structural gray matter volume and response to treatment

We also set up a statistical model to identify significant clusters correlated with response. For this analysis we classified responders based on the decrease of pain at week four compared with the baseline pain. Response was defined as decrease in at least 30% of the pain [35]. Eight amputees were classified as responders (mean percentage pain decrease = 70% ± 26.43). In this model, an unpaired *t*-test was performed using age, gender, TIV, and flipped were included as covariates of no interest to compared difference between responder and non-responder in GMV. The results showed an increase of GMV in two regions in the affected hemisphere in responders compared to non-responders. The two clusters were identified using a TFCE uncorrected *P* values binarized mask at value of .001 and cluster size >27 voxels (Table 2 and Figure 3 uncorrected T-maps, responders > non responders).

Table 1. Demographic and pain characteristics of the amputees

Subject ID	Age	Gender	Side of Amputation	Level of Amputation	Time since Amputation (month)	PLP	RLP	PLS	BDI	Opioid Use
S1	72	M	R	BK	7	6	3	8	5	Y
S2	56	M	L	BK	21	8.5	9	9.5	11	Y
S3	37	F	R	BK	49	2.5	3.5	4	12	N
S4	49	F	L	AK	4	2	2	3	5	Y
S5	45	M	R	AK	389	3.5	4.5	5	29	N
S6	46	F	R	BK	50	4	2	2	7	N
S7	47	F	R	AB	23	6	5	9.5	32	N
S8	52	M	R	BK	163	6.5	5	7	0	N
S9	55	M	R	AK	431	9	8	0	4	N
S10	59	M	L	AD	468	5	1	8	9	Y
S11	21	M	L	BK	160	5	5	3	5	N
S12	64	F	R	BK	21	5.5	0	2	0	N
S13	63	M	R	AK	213	5	0	2	0	Y
S14	53	F	R	PF	4	4.5	0	2	16	N
S15	25	M	L	HD	6	5	5	0	8	Y
S16	69	M	L	BK	6	6	0	0	0	N
S17	59	F	L	BK	5	7	5	8	13	N
S18	60	F	L	AK	7	5	4.5	10	18	Y
S19	32	M	L	AK	4	6	0	10	5	N
S20	61	M	L	AK	6	4	0	4	1	N
S21	57	F	L	BK	456	4	0	3	8	N
S22	77	M	R	BK	285	4	4	9	0	N
S23	46	F	R	BK	4	8	8	8	48	N
S24	38	M	L	BK	4	6	7	5	19	Y

AK = Above the knee (transfemoral); BDI = Beck Depression Inventory; BK = Below the knee; AD = Ankle disarticulation; HD = Hip disarticulation; PF = Partial foot; PLP = Phantom Limb Pain; RLP = Residual Limb Pain; PLS = Phantom Limb Sensation.

Table 2. Clusters showing AIs significantly different from zero in the overall sample

	Region	Number of Voxels	*x*	*y*	*z*	Peak Intensity
Phantom limb pain						
TFCE uncorrected	Insula – NA	471	42	6	−2	6.12
	Frontal Lobe (Subcallosal cortex)	365	8	16	−14	4.49
	Frontal Lobe (Pre-Frontal cortex)	201	6	56	26	4.31
	Thalamus – NAF	37	18	−26	10	3.59
	Thalamus – AF	35	−8	−12	6	4.36
TFCE corrected	Insula -NA	32	42	6	−2	6.12
Responders > Non-Responders						
TFCE uncorrected	Frontal lobe – AF (Primary somatosensory cortex)	112	−52	−18	40	4.34
	Parietal lobe) – AF (Secondary somatosensory cortex)	35	−54	−24	24	4.34

For each cluster, location, aal maps using *fslview*, cluster size, MNI coordinates in mm, and peak intensity values are provided.
AF = affected hemisphere (contralateral to the amputation); NA = not affected hemisphere; TFCE = threshold-free cluster enhancement.

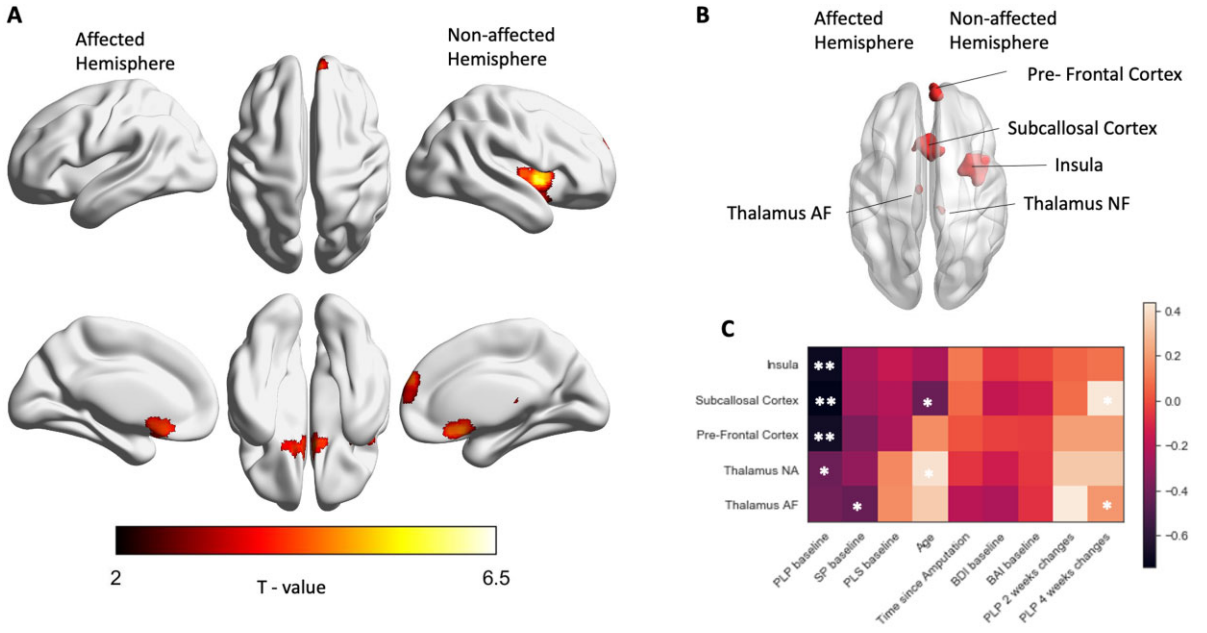

Figure 2. Whole-brain cortical gray matter volume associated with PLP. (**A**) Gray matter morphological volume assessed by voxel-based morphometry (VBM). The twenty-four participants were contrasted together to evaluated positive and negative effect of PLP, with age, gender, and TIV and flipped as covariates of no interest. Shown is the t-value statistical map, clustering determined using TFCE uncorrected *P* values binarized at value of .001 and cluster size < 27 voxels. (**B**) Insula, Subcallosal Cortex, Pre-Frontal Cortex, Thalamus- Affected and Thalamus-Non-Affected hemisphere showed regional GM volume correlated with PLP ($P < .001$, TFCE -uncorrected). (**C**) Correlation between clinical characteristic and brain region volume, color shows Persons correlation coefficients, and $*P < .05$ and $**P < .001$.

Functional decoding

Lastly, we queried the Neurosynth database (neurosynth.org) for a data-driven characterization of our VBM findings using the reverse inference term-based meta-analytic approach [34]. We used the MNI peak coordinates of the insula cluster (Figure 2A; coordinates 42, 6, −2) as the seed region with a threshold of < -0.4 and >0.4 correlation (using a sample of 1000 subjects) to derivate resting-state functional connectivity in Neurosynth [34]. The correlation maps showed that this insula region is highly correlate with itself, the contralateral insula, supplementary motor/pre-motor cortex, and a negative correlated with the precuneus cortex (parietal Lobe) and lateral occipital cortex (Figure 4). Moreover, we used Neurosynth to decode psychological process related with the Insula cluster, presenting the unique terms strongly associated non anatomical terms (Figure 5).

Discussion

Main findings

In this study we showed that alterations of cortical GMV in lower limb amputees with PLP are correlated with phantom pain intensity, but not with other clinical manifestations (PLS, RLS, depression, or anxiety). We found five different clusters in pain-related areas (two in the frontal cortex, two in the thalamus, and one in the insula) that were negatively correlated with PLP intensity (smaller volume associated with higher phantom pain). However, only the insula cluster survived the multiple comparison adjustment—a decrease in the mid-anterior insula cortex volume in the non-affected hemisphere (predominantly from the right side) was correlated with higher PLP. Moreover, the reverse inference meta-analytic approach (Neurosynth) revealed that this mid-anterior insula cluster was highly functional and connected to the

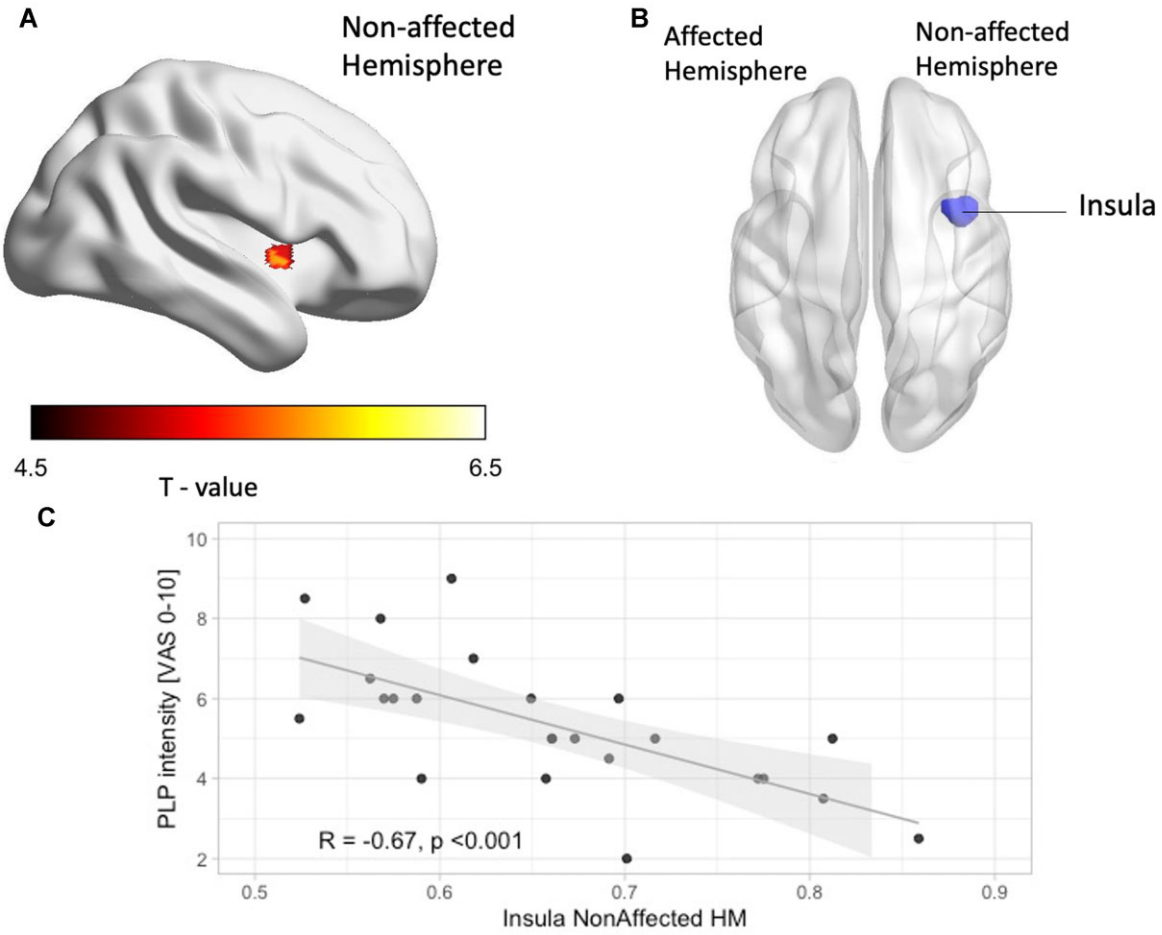

Figure 3. Insula volume of the non-affected hemisphere correlates with PLP. (**A**) Insula gray matter morphological changes assessed by voxel based. The twenty-four participants were contrasted together to evaluated positive and negative effect of PLP, with age, gender, and TIV and flipped as covariates of no interest. Shown is the *t*-test statistical map, clustering determined using TFCE corrected *P* values binarized at value of .05. (**B**) Insula of the Non-Affected hemisphere showed regional GM volume correlated with PLP ($P < .05$, TFCE -corrected). (**C**) Correlation between PLP intensity and insula brain region volume shows strong negative correlation, $P < .001$.

contralateral insular and premotor cortices. Moreover, the decoded psychological processes related to this cluster were "rating," "sustained attention," "impulsivity," and "suffering."

Finally, we showed that responders to neuromodulatory techniques (M1 tDCS and mirror therapy) have different cortical GMV at baseline compared to non-responders. For the responders, we found that somatosensory areas (total volume of S1 and S2) presented more GMV in the affected hemisphere (correspondent to the amputation side) at baseline, compared to non-responders. These results survived multiple comparison adjustment. Interestingly, these alterations were not related with time since amputation and were specific of PLP, since no significant GMV differences were correlated with PLS, RLS, or other phantom phenomena.

PLP severity and gray matter volume of the non-affected hemisphere

Less PLP severity was associated with larger volumes in brain clusters in the non-affected prefrontal (dorsomedial prefrontal cortex and bilateral subcallosal cortex), non-affected insula (mid-anterior region), and bilateral thalamus [36]. Our results are aligned with previous study showing that higher PLP levels were associated with less GMV in the right insula and the caudal portion of the anterior cingulate cortex [19]. These areas are important hubs in the pain connectome being mostly associated with pain control. Their special modulatory tasks such as inhibition/facilitation of pain perception via modulation of the pain descending modulatory system [37] had been associated to other chronic pain conditions including non-neuropathic [15]. Interestingly, no classic motor or somatosensory areas were associated with PLP severity, which had been associated with the presence of PLP [17].

Our results agree with the current theory of the pain connectome where the role of the insula is highlighted during the chronification process [37].This theory proposes that S1 and M1 are only intermediate areas associated to the deafferentation (situation that is to expect); therefore, these pain modulatory regions need to be target directly or indirectly in future interventions. Therefore, the data suggest that two different neural networks are in play: brain circuits for PLP generation, and circuits for PLP persistence/severity.

On one hand, we hypothesize that higher GMV of pain control areas is associated with higher neural recruitment of these modulatory networks in subjects post amputation. Consequently, patients with better adaptation to deafferentation and less central sensitization recruit more pain control related areas (indexed by high GMV in these areas) and have

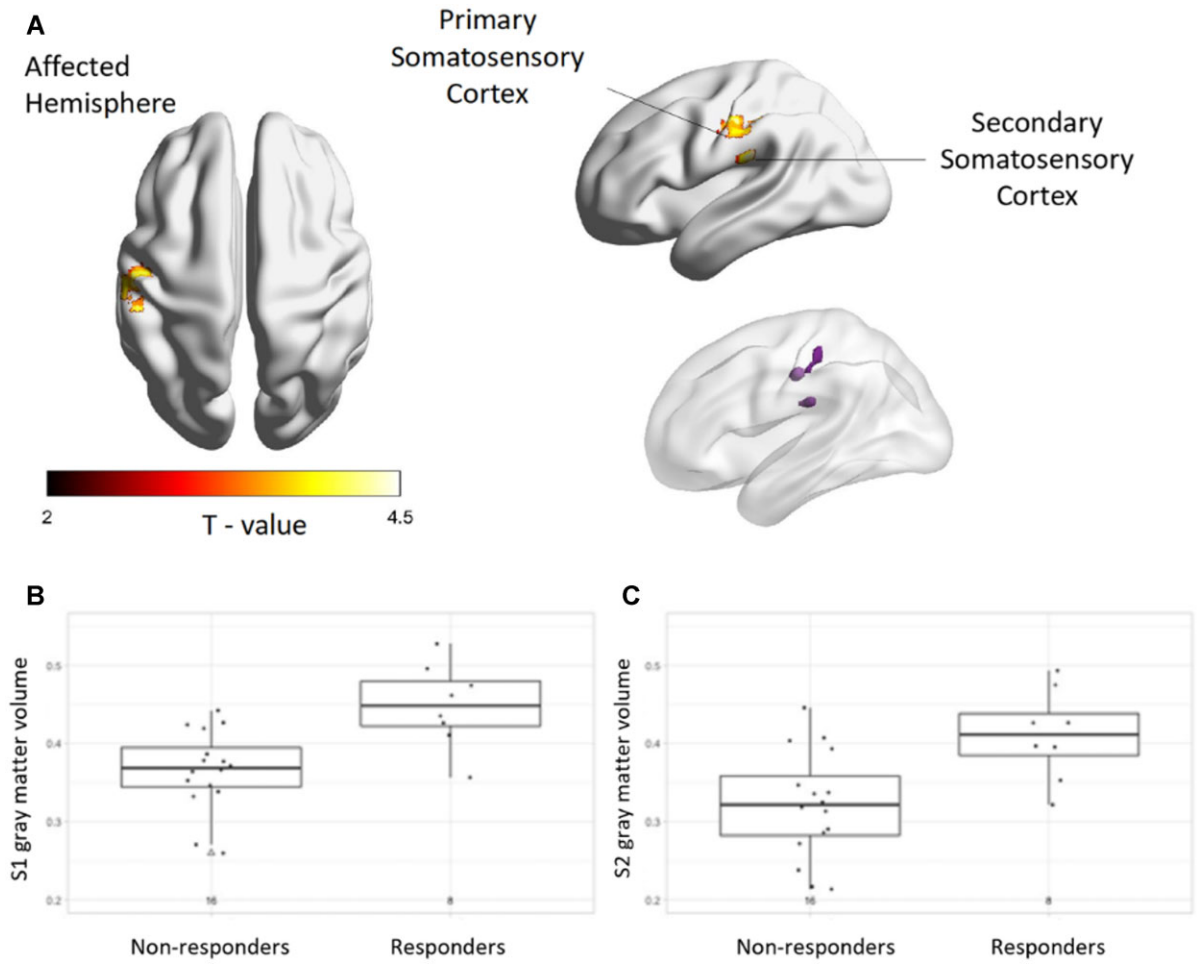

Figure 4. Differences in GMV between responders and non-responders. (**A**) Primary and secondary somatosensory cortex gray matter volume increases in responders compared with non-responders both in the affected hemisphere. Compared with non-responders, responders showed GMV increase of volume in the somatosensory cortex. Conversely, no brain regions showed greater GMV in non-responders compared with responders at this threshold. Shown is the *t*-test statistical map, clustering determined using TFCE uncorrected *P* values binarized value of .001 and cluster size >27 voxels. (**B**) Primary somatosensory cortex of the Affected hemisphere showed regional increase in GM volume (Kruskal-Wallis test $P < .05$). (**C**) Secondary somatosensory cortex of the Affected hemisphere showed regional increase in GM volume (Kruskal-Wallis test $P < .05$).

lower PLP levels. This is supported by studies on neurorehabilitation showing that cognitive and sensorimotor training induced higher specific neural recruitment reflected as increased cortical GM thickness in areas related to the training [20, 38]. However, longitudinal assessments of phantom phenomena trajectories are needed to confirm our hypothesis. For instance, large populational longitudinal cohorts as the United Kingdom biobank [39], or the Denmark birth cohort [40] could include neuroimaging protocols in the registry system for those cases that develop during the follow-up period a risk for a programmed amputation (new-onset cancer patients or de novo vascular complications). These assessments should start before amputation, right after amputation, and then follow up the appearance, persistence, and severity of PLP using clinical evaluations and structural and functional neuroimaging.

On the other hand, the classic persistence or reorganization of the contralateral somatosensory and motor areas [41] are consistently reported in studies comparing amputees with PLP and healthy subjects, but not when analyzing the clinical severity of the disease. Thus, we hypothesized that these modifications represent a neural characteristic of presence/generation of PLP, likely due to maladaptation to deafferentation and anomalous spinal and peripheral input inducing a thalamic disorganization and subsequent cortical changes. However, not necessarily maintaining a persistent chronic pain state, likely the interplay with pain control areas is needed to induce chronic PLP. This is further supported by Kikkert et al. (2018) [13] study; the authors found that PLP level was associated with hyperactivity and hyperconnectivity between sensorimotor (S1/M1) and pain regulatory areas such as the insula. As a result, the optimization of current PLP treatments need to focus on modifying the neural networks associated with PLP persistence/severity and its multifocal dynamic nature (hyperconnectivity between pain control hubs during phantom activity) instead of only targeting disorganization of sensory maps. An emerging alternatives include phantom motor execution (42) and non-invasive brain stimulation such as tDCS [9, 13, 24, 43].

Furthermore, most of the associated GMV differences are from areas in the non-affected hemisphere. This suggests a hemispheric control of PLP that goes beyond the hemisphere contralateral to the amputation. The integration of ipsilateral neural networks to the amputation are likely compensating to

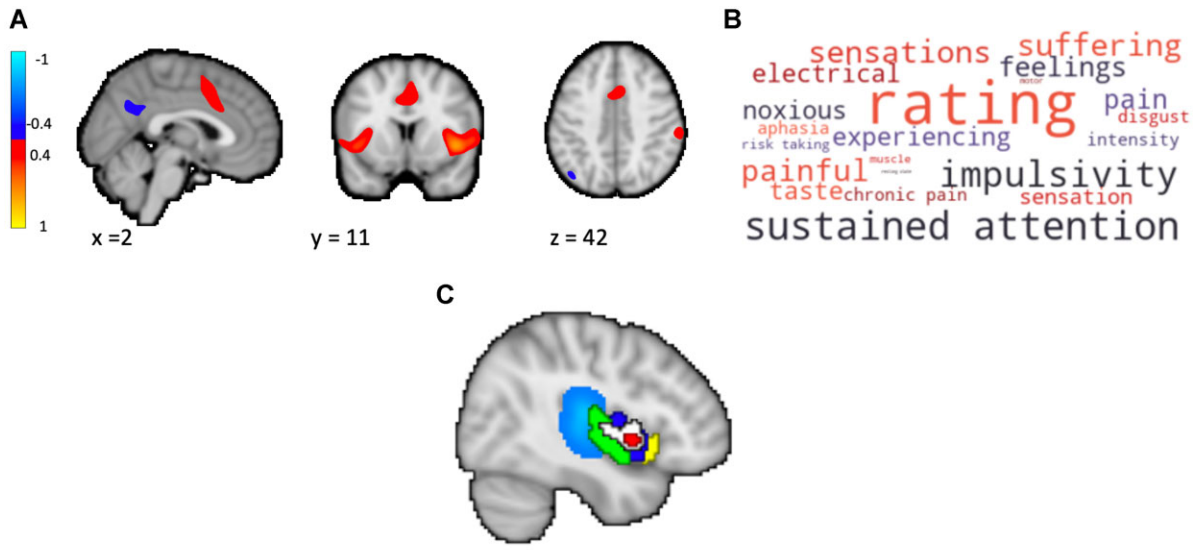

Figure 5. Neurosynth resting-state functional connectivity for the insula cluster. **(A)** A location seed used to identify functional connectivity of the Insula region (coordinates: 42, 6, −2) with the rest of the brain using reverse inference maps from Neurosynth. Functional connectivity map shows activity synchronization with bilateral insula cortex, supplementary motor/pre-motor cortex, precuneus cortex, and lateral occipital cortex, when connectivity is thresholded to < -0.4 and > 0.4. **(B)** Neurosynth database terms associated with the insula cluster show a stronger association with "rating," "sustained attention," "impulsivity," "suffering," "sensations" and "painful"; World cloud represents the top non-anatomical terms, the sizes of words correspond to the Pearson correlation coefficient from Neurosynth. Images are not in radiological convention. **(C)** Anatomical representation of the found insula cluster (coordinates: 42, 6, −2), in red corrected voxels, in white uncorrected voxels. The cluster is predominantly in the mid-anterior insula.

the maladaptive plasticity of the affected hemisphere. This is supported by current evidence on the bilateral involvement of pain perception integration and control [36].

The role of insula in PLP severity at baseline

The most robust finding associated with PLP severity is the role of the non-affected mid-anterior insula (predominantly from the right side). Several pain conditions have been associated with alteration in the insula [44]. The current literature supports the hypothesis that nociceptive informationis processed in succession along the insula, along the posterior–anterior axis, each segment related to a different dimension of pain—posterior insula adding sensory-discriminatory integration, and mid-anterior insula integrating affective-motivational and cognitive-evaluative aspects of pain perception—becoming fully integrated in the anterior insula [45, 46]. This is supported by our reverse inference meta-analytic approach which showed that the insula cluster we found has activity synchronization with the bilateral insula, supplementary motor/pre-motor cortex, precuneus cortex, and lateral occipital cortex—areas from different sensorial modalities related to pain perception. Additionally, the term-based cloud obtained from Neurosynth revealed association with "rating," "sustained attention," "impulsivity," and "suffering," confirming the perceptual integrative role of the insula cluster we found associated with PLP severity. Likewise, a recent study showed higher insula hyperconnectivity during phantom hand imagination associated with PLP and treatment response [13]. Therefore, taken together, the results support the central role of mid-anterior insula in chronic PLP perception and its severity, likely based on the degree of coordinated connectivity to integrate pain perception. Although, hypothetical, we could expect a relationship between an organized and adaptive insula functioning with some degree of gray matter increase, which could explain our results.

Furthermore, another explanation to our findings is the role of the insula in the multimodal sensory stimulus salience detection network, where salience stimuli are encoded and processed to appropriately orient attention [47, 48]. Given that chronic pain is inherently salient, it is possible that the changes detected could reflect the salience of the stimulus and the appropriate attention allocation to the painful stimulus [49]. Future studies will need to investigate structural and functional brain characteristics during attentional tasks in PLP to understand overlapping mechanisms.

Gray matter volume associated with dynamic PLP changes associated with neuromodulation treatment

We found that higher gray matter volume in somatosensory cortices (total volume of S1 and S2) of the affected hemisphere at baseline are associated with PLP reduction after M1 tDCS and mirror therapy interventions. Only few studies have explored biomarkers of treatment response in PLP. One study found that increased activity in the non-affected mid insula and S2 cortex during the tDCS stimulation predicted PLP relief after 90 minutes; this activity change, consequently, produced a reduction of S1-insula connectivity and modification of S1/M1 activity [13]. These results are consistent with our findings, supporting the idea of target engagement of S1/M1 tDCS to treat PLP, brain region that is potentially acting as an entry port for further modulation of pain control networks such as insula integration [50]. In our case we combined M1 tDCS with a motor representation technique (mirror therapy) which likely produced a higher sensorimotor engagement during the treatment sessions. We hypothesized that patients with higher GMV in S1/S2 can recruit easily brain resources to better adapt and revert maladaptive plasticity post-amputation induced by neuromodulatory interventions. This is supported by our recent clinical trial showing changes on intracortical inhibition and readaptation of motor cortex representation using TMS [24]; also, we have found that higher phantom

movement sensations—a non-painful phenomenon—acted as protective factor and could predict treatment response [11, 51]. Taken all together, the evidence suggests that the heterogeneity of motor cortex neuromodulatory interventions in PLP can be explained by sensorimotor cortex structural and connectivity differences. This is highly significant to optimized current neuromodulatory techniques and to start implementing a personalized management approach in PLP.

The specificity of gray matter volume findings

Other assessment of clinical severity such as PLS, RLP, depression, and anxiety, were not associated with GMV differences. Likewise, GMV at baseline could not predict the improvement of other clinical variables after treatment. This suggests that non-painful and emotion-related symptoms after amputation are not necessarily depending on gray matter volume and the structural correlates are minimal. Further exploration using functional imaging is needed to assess neurophysiological correlates of these clinical components of the disease severity.

Strengths and limitations

We performed a comprehensive GMV exploration using high-definition voxel-based morphometry methods and functional decoding using a reverse inference term-based meta-analytic approach to understand the structural neuroimaging correlates of PLP severity and treatment response. Also, we studied a homogenous sample in terms of localization and the etiology of etiology (unilateral, traumatic, lower-limb amputees), increasing the internal validity of our results. Nevertheless, our study had some limitations. The analysis was limited to volume differences, but no functional activity or connectivity; thus, our results should be interpreted with caution considering that GMV differences are not necessarily associated with brain activity. In addition, the range of time since amputation was relatively large. Since most of our participants were only examined years after amputation, we have no information about gray matter trajectories across time. Finally, PLP ratings using VAS one day cannot capture the oscillating nature of PLP severity, further validation of our GMV findings is needed with longitudinal assessments of pain starting at the time of amputation.

Conclusion

Gray matter volume was negatively associated with PLP intensity but no other clinical manifestations. The volume differences were present in the non-affected hemisphere (ipsilateral to the amputation) suggesting a compensatory mechanism to maladaptive plasticity post amputation. The mid-anterior insula is an important structural hub associated with the PLP severity and likely this represents its modulatory and integrating function of pain perception in these patients. Moreover, patients with higher gray matter in the somatosensory cortices had higher PLP reduction after non-invasive motor cortex neuromodulatory treatment. Our data suggest that gray matter volumetric analysis can be applied to understand the pathophysiology behind the PLP severity and to endotype PLP treatment responders based on their gray matter patterns. Future applications of these findings can be used to validate biomarkers and improve treatment allocation.

Supplementary material

Supplementary material is available at *Pain Medicine* online.

Funding

This work is supported by a National Institutes of Health (NIH) grant (R01-HD082302-01A1).

Conflicts of interest: No conflict of interest to declare. This study was developed in the absence of any commercial or financial relationships that could be construed as a potential conflict of interest.

References

1. Ziegler-Graham K, MacKenzie EJ, Ephraim PL, Travison TG, Brookmeyer R. Estimating the prevalence of limb loss in the United States: 2005 to 2050. Arch Phys Med Rehabil. 2008;89(3):422-429.
2. Limakatso K, Bedwell GJ, Madden VJ, Parker R. The prevalence and risk factors for phantom limb pain in people with amputations: a systematic review and meta-analysis. PLoS One. 2020;15 (10):e0240431.
3. Hanyu-Deutmeyer AA, Cascella M, Varacallo M. Phantom limb pain. In: Hauber S, Dulebohn S, eds. StatPearls. StatPearls Publishing; 2021:1–5.
4. Limakatso K, Parker R. Treatment recommendations for phantom limb pain in people with amputations: an expert consensus Delphi study. PM R. 2021;13(11):1216-1226.
5. Hanley MA, Ehde DM, Campbell KM, Osborn B, Smith DG. Self-reported treatments used for lower-limb phantom pain: descriptive findings. Arch Phys Med Rehabil. 2006;87(2):270-277.
6. Aternali A, Katz J. Recent advances in understanding and managing phantom limb pain. F1000Research. 2019;8:1167.
7. Urits I, Seifert D, Seats A, et al. Treatment strategies and effective management of phantom limb–associated pain. Curr Pain Headache Rep. 2019;23(9):1-7.
8. Browne JD, Fraiser R, Cai Y, Leung D, Leung A, Vaninetti M. Unveiling the phantom: what neuroimaging has taught us about phantom limb pain. Brain Behav. 2022;12(3):e2509.
9. Duarte D, Bauer CCC, Pinto CB, et al. Cortical plasticity in phantom limb pain: an fMRI study on the neural correlates of behavioral clinical manifestations. Psychiatry Res Neuroimaging. 2020; 304:111151.
10. Makin TR, Scholz J, Filippini N, Henderson Slater D, Tracey I, Johansen-Berg H. Phantom pain is associated with preserved structure and function in the former hand area. Nat Commun. 2013;4(1):8,
11. Gunduz ME, Pinto CB, Saleh Velez FG, et al. Motor cortex reorganization in limb amputation: a systematic review of TMS motor mapping studies. Front Neurosci. 2020;14:314.
12. Pacheco-Barrios K, Pinto CB, Velez FGS, et al. Structural and functional motor cortex asymmetry in unilateral lower limb amputation with phantom limb pain. Clin Neurophysiol. 2020;131 (10):2375-2382.
13. Kikkert S, Mezue M, O'Shea J, et al. Neural basis of induced phantom limb pain relief. Ann Neurol. 2019;85(1):59-73.
14. Scarpazza C, De Simone MS. Voxel-based morphometry: current perspectives. NAN. 2016;5:19-35.
15. Cauda F, Palermo S, Costa T, et al. Gray matter alterations in chronic pain: a network-oriented meta-analytic approach. Neuroimage Clin. 2014;4:676-686.
16. Smallwood RF, Laird AR, Ramage AE, et al. Structural brain anoMalies and chronic pain: a quantitative meta-analysis of gray matter volume. J Pain. 2013;14(7):663-675.
17. Draganski B, Moser T, Lummel N, et al. Decrease of thalamic gray matter following limb amputation. Neuroimage. 2006;31(3):951-957.

18. Preißler S, Dietrich C, Blume K, Hofmann GO, Miltner WHR, Weiss T. Plasticity in the visual system is associated with prosthesis use in phantom limb pain. Front Hum Neurosci. 2013;7:311.
19. Preissler S, Feiler J, Dietrich C, Hofmann GO, Miltner WHR, Weiss T. Gray matter changes following limb amputation with high and low intensities of phantom limb pain. Cereb Cortex. 2013;23(5):1038-1048.
20. Preißler S, Thielemann D, Dietrich C, Hofmann GO, Miltner WHR, Weiss T. Preliminary evidence for training-induced changes of morphology and phantom limb pain. Front Hum Neurosci. 2017;11:319.
21. Sinha R, van den Heuvel WJA, Arokiasamy P. Factors affecting quality of life in lower limb amputees. Prosthet Orthot Int. 2011;35 (1):90-96.
22. Pacheco-Barrios K, de Melo PS, Vasquez-Avila K, et al. Accelerating the translation of research findings to clinical practice: insights from phantom limb pain clinical trials. Princ Pract Clin Res. 2021;7(4):1-7.
23. Pinto CB, Saleh Velez FG, Bolognini N, Crandell D, Merabet LB, Fregni F. Optimizing rehabilitation for phantom limb pain using mirror therapy and transcranial direct current stimulation: a randomized, double-blind clinical trial study protocol. JMIR Res Protoc. 2016;5(3):e138.
24. Gunduz ME, Pacheco-Barrios K, Bonin Pinto C, et al. Effects of combined and alone transcranial motor cortex stimulation and mirror therapy in phantom limb pain: a randomized factorial trial. Neurorehabil Neural Repair. 2021;35(8):704-716.
25. Kooijman CM, Dijkstra PU, Geertzen JHB, Elzinga A, Van der Schans CP. Phantom pain and phantom sensations in upper limb amputees: an epidemiological study. Pain. 2000;87 (1):33-41.
26. Jenkinson M, Beckmann CF, Behrens TE, Woolrich MW, Smith SM. FSL. Neuroimage. 2012;62(2):782-790.
27. Greve DN. An absolute beginner's guide to surface-and voxel-based morphometric analysis. Proceedings of the International Society for Magnetic Resonance in Medicine 2011;19:33.
28. Jenkinson M, Bannister P, Brady M, Smith S. Improved optimization for the robust and accurate linear registration and motion correction of brain images. Neuroimage. 2002;17(2):825-841.
29. Jlrjm A. Non-linear registration, aka spatial 524 normalisation, FMRIB Tech Rep TR07JA2 2010, 2010.
30. Nichols TE, Holmes AP. Nonparametric permutation tests for functional neuroimaging: a primer with examples. Hum Brain Mapp. 2002;15(1):1-25.
31. Smith SM, Nichols TE. Threshold-free cluster enhancement: addressing problems of smoothing, threshold dependence and localisation in cluster inference. Neuroimage. 2009;44(1):83-98.
32. Barroso J, Vigotsky AD, Branco P, et al. Brain grey matter abnorMalities in osteoarthritis pain: a cross-sectional evaluation. Pain. 2020;161(9):2167-2178.
33. Smith SM, Jenkinson M, Woolrich MW, Beckmann CF, et al. Advances in functional and structural MR image analysis and implementation as FSL. Neuroimage. 2004;23(Suppl 1): S208-S219.
34. Yarkoni T, Poldrack RA, Nichols TE, Van Essen DC, Wager TD. Large-scale automated synthesis of human functional neuroimaging data. Nat Methods. 2011;8(8):665-670.
35. Dworkin RH, Turk DC, Wyrwich KW, et al. Interpreting the clinical importance of treatment outcomes in chronic pain clinical trials: IMMPACT recommendations. J Pain. 2008;9(2):105-121.
36. Kucyi A, Davis KD. The dynamic pain connectome. Trends Neurosci. 2015;38(2):86-95.
37. Huynh V, Lütolf R, Rosner J, et al. Descending pain modulatory efficiency in healthy subjects is related to structure and resting connectivity of brain regions. Neuroimage. 2022;247:118742.
38. Liepert J, Miltner WH, Bauder H, et al. Motor cortex plasticity during constraint-induced movement therapy in chronic stroke patients. Neurosci Lett. 1998;250(1):5-8.
39. Bycroft C, Freeman C, Petkova D, et al. The UK Biobank resource with deep phenotyping and genomic data. Nature. 2018;562 (7726):203-209.
40. Olsen J, Melbye M, Olsen SF, et al. The Danish National Birth Cohort–its background, structure and aim. Scand J Public Health. 2001;29(4):300-307.
41. Makin TR, Flor H. Brain (re) organisation following amputation: implications for phantom limb pain. Neuroimage. 2020;218: 116943.
42. Ortiz-Catalan M, Gumundsdóttir RA, Kristoffersen MB, et al. Phantom motor execution facilitated by machine learning and augmented reality as treatment for phantom limb pain: a single group, clinical trial in patients with chronic intractable phantom limb pain. Lancet. 2016;388(10062):2885-2894.
43. Fregni F, El-Hagrassy MM, Pacheco-Barrios K, et al.; Neuromodulation Center Working Group. Evidence-based guidelines and secondary meta-analysis for the use of transcranial direct current stimulation in neurological and psychiatric disorders. Int J Neuropsychopharmacol. 2021;24(4):256-313.
44. Moayedi M. All roads lead to the insula. Pain. 2014;155 (10):1920-1921.
45. Farmer MA, Baliki MN, Apkarian AV. A dynamic network perspective of chronic pain. Neurosci Lett. 2012;520(2):197-203.
46. Frot M, Faillenot I, Mauguière F. Processing of nociceptive input from posterior to anterior insula in humans. Hum Brain Mapp. 2014;35(11):5486-5499.
47. Downar J, Crawley AP, Mikulis DJ, Davis KD. A cortical network for the detection of novel events across multiple sensory modalities. Neuroimage. 2001;13(6):310.
48. Downar J, Crawley AP, Mikulis DJ, Davis KD. A cortical network sensitive to stimulus salience in a neutral behavioral context across multiple sensory modalities. J Neurophysiol. 2002;87(1):615-620.
49. Downar J, Mikulis DJ, Davis KD. Neural correlates of the prolonged salience of painful stimulation. Neuroimage. 2003;20 (3):1540-1551.
50. Pacheco-Barrios K, Cardenas-Rojas A, Thibaut A, et al. Methods and strategies of tDCS for the treatment of pain: current status and future directions. Expert Rev Med Devices. 2020;17(9):879-898.
51. Münger M, Pinto CB, Pacheco-Barrios K, et al. Protective and risk factors for phantom limb pain and residual limb pain severity. Pain Pract. 2020;20(6):578-587.